The Supporting Information

Interface Engineering of Semiconductor/Dielectric Heterojunctions toward Functional Organic Thin-Film Transistors

Hongtao Zhang,[1,2] Xuefeng Guo,*[3,4] Jingshu Hui,[3] Shuxin Hu,[5]
Wei Xu,[1] and Daoben Zhu*[1]

[1]Key Laboratory of Organic Solids, Beijing National Laboratory for Molecular Science, Institute of Chemistry, Chinese Academy of Sciences, Beijing 100190, P. R. China.

[2]Graduate School of Chinese Academy of Sciences, Beijing 100049, P. R. China.

[3]Center for Nanochemistry, Beijing National Laboratory for Molecular Sciences (BNLMS), State Key Laboratory for Structural Chemistry of Unstable and Stable Species, College of Chemistry and Molecular Engineering, Peking University, Beijing 100871, P. R. China.

[4]Department of Advanced Materials and Nanotechnology College of Engineering, Peking University, Beijing 100871, P. R. China

[5]Institute of Physics, Chinese Academy of Sciences, Beijing 100190, P. R. China.

*Email: guoxf@pku.edu.cn; zhudb@iccas.ac.cn

Experimental Section

Materials. A spiropyran carboxylic acid (**2**) was straightforwardly synthesized as shown in Scheme 1. Pentacene and $F_{16}CuPc$ were purchased from the Aldrich Corporation and used after further sublimation purification. Polymethyl methacrylate (PMMA) (M_n = 495 Kg/mol, A6) was purchased from Microchem Corporation and used as received. N,N-dihexylperylene diimide (PEDI) was prepared according to the reference.[1] Other chemical reagents for synthesis were purchased from Aldrich Chemical Co. unless otherwise indicated. UV-Vis spectra were recorded on Perkin Elmer Lambda35 UV-Vis spectrophotometer. X-ray photoelectron spectroscopy data of SP-SAM were obtained with an ESCALab220i-XL electron spectrometer from VG Scientific using 300W AlKα radiation. The base pressure was about 3×10^{-9} mbar. The binding energies were referenced to the C1s line at 284.8 eV from adventitious carbon. The water contact angles were obtained from dataphysics OCA-20 contact angle instrument. IR spectra were recorded on a Nicolet ECTOR22 FT-IR. X-ray reflectivity data were obtained from Bruker D8-Advance diffractometer.

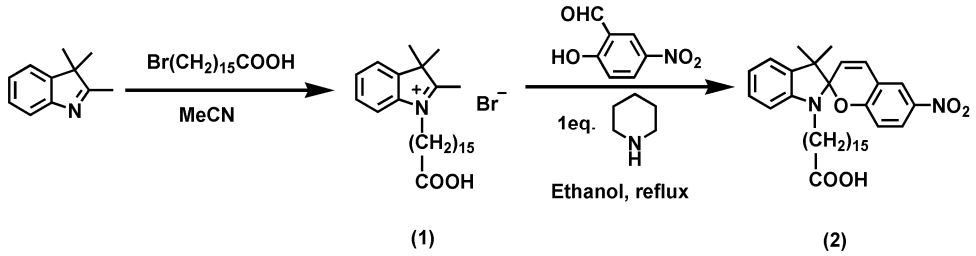

Scheme 1. Synthetic route for a spiropyran carboxylic acid.

Synthesis of spiropyran carboxylic acid (2). *Synthesis of N-(16-Carboxyhexadecyl)-2,3,3-trimethylindolenium bromide (**1**).* 1,16-Bromohexa- decanoic (3.34 g, 10 mmol) and 2,3,3-trimethylindolenin (1.58 ml, 10 mmol) were dissolved in 5 mL of

acetonitrile and refluxed for 72 h. After cooling down to room temperature, the solution was evaporated under reduced pressure. The solid formed was precipitated with ether three times to give red-purple solid of **1** (3.09 g, 7.47 mmol) in 74.7% yield. This compound was used in the next step without any further purification. ^{1}H NMR (300 MHz, DMSO-d_6, δ): 7.98 (m, 1H, CH), 7.85 (m, 1H, CH), 7.62 (m, 2H, CH), 4.45 (t, 2H, CH_2), 2.84 (s, 3H, CH_3), 2.18 (t, 2H, CH_2), 1.84 (m, 2H, CH_2), 1.53 (s, 6H, CH_3), 1.47 (m, 2H, CH_2), 1.23 (m, 22H, CH_2). MS (ESI, m/z): 414.3 [M^+ – Br].

*Synthesis of 1′-(16′-Carboxyhexadecyl)-3′,3′-dimethyl-6-nitrospiro[2H-1]benzo-pyran-2,2′-indoline (**2**).* Compound **1** (749 mg, 1.51 mmol) and 5-nitrosalicylaldehyde (304 mg, 1.82 mmol) were dissolved in 20 mL of ethanol. Triethylamine (0.25 mL) was added to the ethanol solution over 30 mins. After 8 h reflux, the reaction solution was cooled down to room temperature. The precipitate was filtered. The obtained solid was recrystallized from ethanol three times to give yellow crystals of **2** (524 mg, 0.932 mmol) in 61.7% yield. ^{1}H NMR (300 MHz, $CDCl_3$, δ): 8.02 (d, 1H, CH), 7.98 (d, 1H, CH), 7.18 (m, 1H, CH), 7.07 (dd, 1H, CH), 6.89 (d, 1H, CH), 6.83 (m, 1H, CH), 6.73 (d, 1H, CH), 6.56 (d, 1H, CH), 5.85 (d, 1H, CH), 3.13 (m, 2H, CH_2), 2.35 (t, 2H, CH_2), 1.58-1.65 (m, 4H, CH_2), 1.17-1.22 (m, 28H, CH_2+CH_3). MS (ESI, m/z): 563.3 [M^+ + H].

Formation of SP SAMs. SP SAMs were formed on SiO_2 substrates in two steps as described previously.[2-3] Before forming SAMs, the SiO_2 substrates underwent a hydrophilic treatment by heating to 110℃ in a Piranha solution for 0.5 h. The (3-aminopropyl)-trimethoxysilane (APTMS) SAMs were formed by immersing

cleaned substrates in freshly mixed 94% acidic methanol (1.0 mM acetic acid in methanol), 5.0% H_2O, and 1.0% APTMS for 15 min at room temperature and then rinsing three times in methanol.[4] Following the final rinse step in APTMS preparations, slides were baked on a hotplate at 120℃ for 5 min. The baking step was performed to quickly remove residual solvent and promote the complete reaction of the silanes. After the formation of the APTMS SAMs, slides were immersed in the fresh 1mM SP **2**/toluene solution, which contains 0.1% DCC inside, at room temperature for 3 days. The toluene agent was freshly purified by Sodium/benzophenone. After monolayer formation, the samples were washed three times with copious toluene.

Device Fabrication and Characterization. After monolayer formation, pentacene films (40 nm) were fabricated on top of the SAMs by thermal evaporation at a base pressure of 2×10^{-6} Torr with a rate of 0.1 $A\cdot s^{-1}$. Drain and source electrodes (50 nm Au) were deposited on the surface of the semiconductor layer through a shadow mask at a base pressure of 3×10^{-6} Torr. The resulting channel length and width were 60 μm and 7 mm, respectively. Pentacene films were analyzed by atomic force microscopy (AFM) using a Nanoscope IIIA Scanning Probe Microscope with silicon cantilevers in the tapping mode.

The capacitance of the hybrid dielectric films was measured on the sandwich electrode structures with gold pads (0.9 mm^2) using a Karl Suss probe station equipped with a digital capacitance meter (Agilent 4294A). The devices were characterized with the same probe station and semiconducting parameter analyzer

(Agilent 4155C). Carrier mobilities (μ) were calculated in the saturation regime by the standard method: $I_D = WC_i\mu(V_G-V_T)^2/(2L)$, where I_D is the source-drain saturation current, C_i is the gate dielectric capacitance (per area), V_G is the gate voltage, and V_T is the threshold voltage. V_T can be estimated as the x intercept of the linear section of the plot of V_G vs. $(I_D)^{1/2}$. Light irradiations were performed with a handheld UV lamp (~ 10 μW/cm^2, λ = 365 nm) and with a 150 W Halogen incandescent lamp (I_{max} = ~ 30 mW/cm^2, λ > 520 nm). To avoid the heating effect during irradiation, visible light was focused and guided by a long optical fiber to the probe station. To aid in the analysis of the results, we intend to regulate the intensity of visible light that makes the photocurrents of the devices under visible irradiation equivalent to those induced by UV irradiation. By doing this, we can record the time trace of the drain currents of the devices without obvious current jumps when UV and visible lights are switched. All of the measurements were consistently performed in the same condition and at the same temperature.

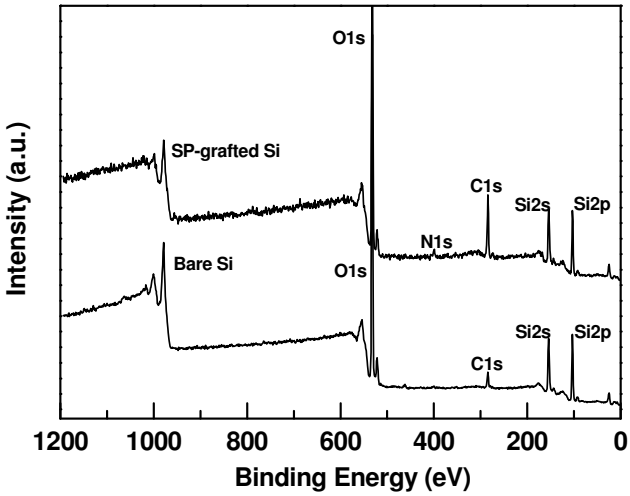

Figure S1. Wide scan XPS spectra (survey) of a SP-grafted SiO_2 wafer as compared to the same substrate before two-step functionalizations.

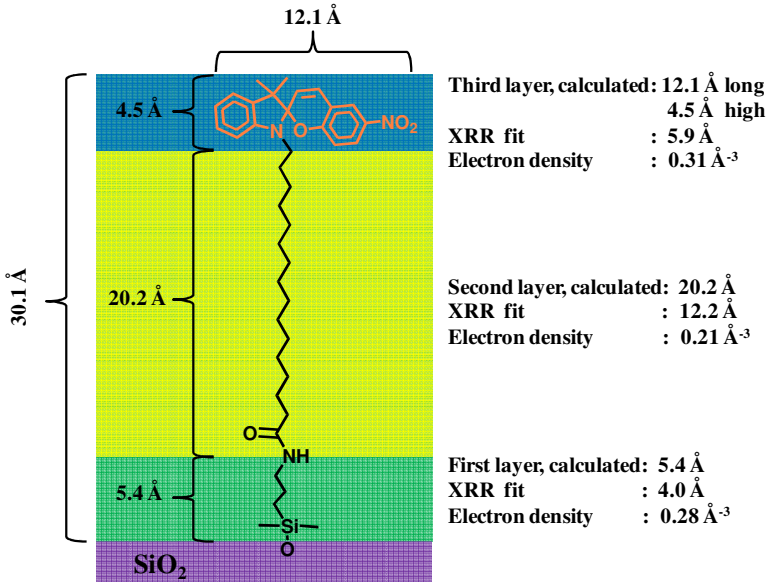

Figure S2. The chemical structure of SP SAMs and the thickness and electron densities obtained from the fit in Fig. 2c.

UV-vis spectroscopy

UV-vis spectroscopy was used to determine the monolayer density on thin fused quartz substrates. If we assume a uniform distribution on the surface and that the extinction coefficient in solution and in a monolayer is the same we can relate the

absorbance spectra with a calculated surface density. The monolayer surface concentration is given by c = A/(2*ε*b) [M], where the factor of 2 in the denominator accounts for the functionalization of both sides of the quartz substrate. The figure below is a plot depicting the molar extinction coefficient for a solution of 1.0×10^{-5} M and the absorbance of a monolayer film. The peak at 336 nm gives a molar extinction coefficient of 9.4×10^{3} $M^{-1} \cdot cm^{-1}$. The monolayer absorbance for this sample was about 5.5×10^{-3}, which translates to a concentration of 1.32 M or 1.8×10^{14} molecules/cm^2. The closed packed molecular surface coverage estimation, 2.0×10^{14} molecules/cm^2, was determined by calculating area covered by a SP individual molecule, that is tilted by an angle of 42.8 degrees on the surface (Fig. 2d), with dimensions of 1.21 nm long and 0.56 nm wide.

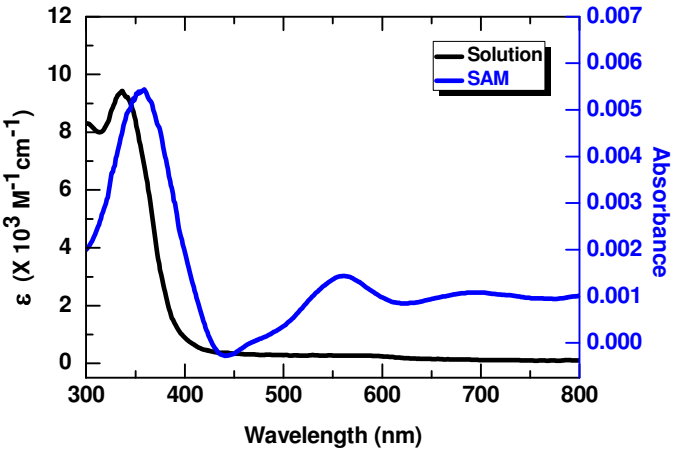

Figure S3. Comparison of the UV-vis spectra of a solution of SP (black curve, left axis) in THF (1.0×10^{-5} M) and a monolayer film of SP on quartz (blue curve).

Calculation Method for the Percent Conversion of SP Molecules

Photochromism is defined as a reversible change in a chemical species between two forms.

$$\mathbf{A} \underset{K_{(visible)} + k_{(dark)}}{\overset{K_{(UV)}}{\rightleftharpoons}} \mathbf{B}$$

To calculate the percent conversion (x) of SP molecules from SP-close (**A**) to SP-open (**B**), a semiempirical approach is used, assuming that a pseudo-first-order process with linear intensity dependence adequately describes the present photochromic system (Berkovic, G.; Krongauz, V.; Weiss, V. *Chem. Rev.* **2000**, *100*, 1741). In solid polymer, the thermal conversion from SP-close (**A**) to SP-open (**B**) may be neglected. SP-open (**B**) may be a mixture of several stereoisomers of the merocyanine form and their aggregates. Then the overall change in concentration of SP-open (**B**) with time can be simply given by the following rate equation: $-dB/dt = K_{(visible)}B - K_{(UV)}A + K_{(dark)}B = K_{(visible)}\,A_0x - K_{(UV)}A_0(1 - x) + K_{(dark)}\,A_0x$ where A and B are the concentrations of SP-close and SP-open, $K_{(UV)}$ and $K_{(visible)}$ are the photochemical rate constants, $K_{(dark)}$ is the thermal rate constant for conversion from SP-open to SP-close, and A_0 is the total concentration of all the SP molecules. At the photostationary state, the percent conversion (x_e) of SP molecules from SP-close to SP-open can be calculated through the following relationship:

$$\frac{x_e}{1-x_e} = \frac{K_{(UV)}}{K_{(Visible)} + K_{(dark)}}$$

In the case of SP SAMs discussed in the main text, the rate contants for each process are calculated, $K_{(UV)} = \sim 0.31\ s^{-1}$, $K_{(visible)} = \sim 5.5 \pm 0.1 \times 10^{-2}\ s^{-1}$, and $K_{(dark)} = \sim 1.1 \pm 0.1 \times 10^{-3}\ s^{-1}$ (data in the dark unshown) (Figure S3). As a result, the calculated percent conversion (x_e) of SP molecules from SP-close to SP-open at the photostationary state is ~ 84.4%.

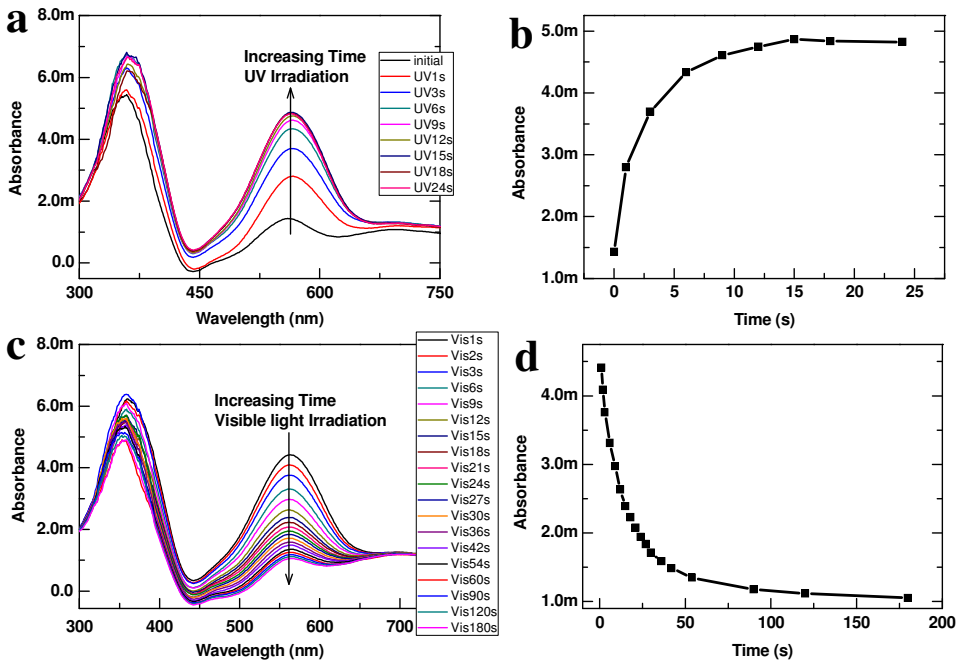

Figure S4. The gradual transitions of the UV/visible absorption spectra of a SP SAM on a quartz substrate under UV (a and b) and visible light (c and d) irradiation.

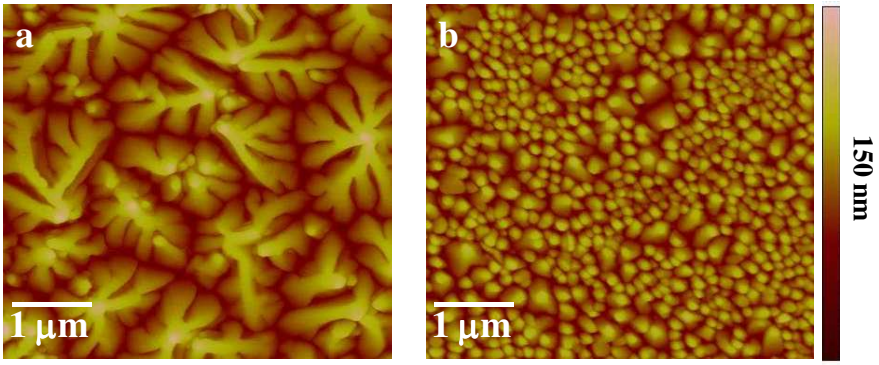

Figure S5. Representative tapping-mode AFM images obtained from 40-nm pentacene thin films grown on bare SiO_2 substrates (a) and SP SAM-SiO_2 hybrid substrates (b).

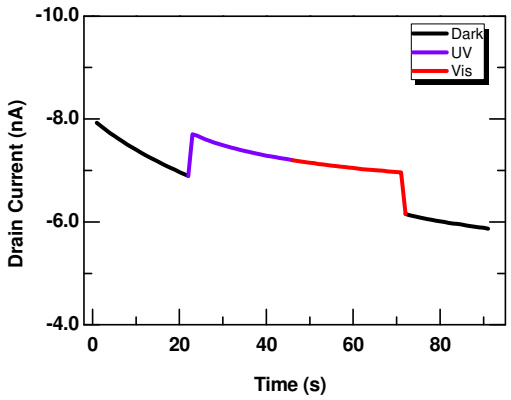

Figure S6. Time trace of the drain current for a control device on APTMS-treated silicon substrates that lacks SP SAMs under irradiation of UV light (365 nm) and visible light (λ > 520 nm). V_D = -30 V, V_G = -15 V.

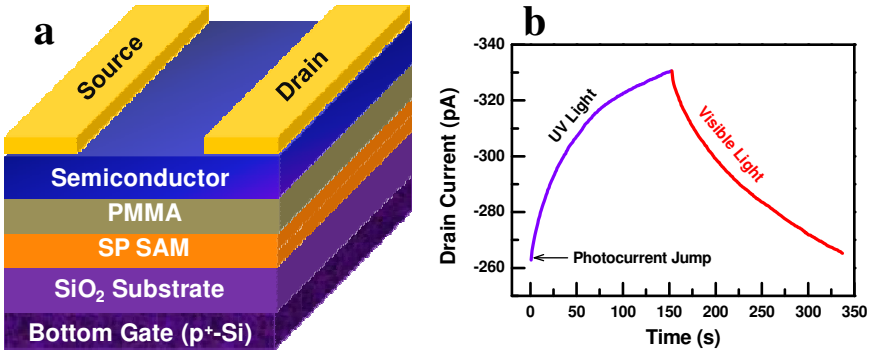

Figure S7. (a) Structural representation of a device built on SP SAMs that were covered by PMMA thin films. (b) The time-dependent behavior of such a device under UV and visible light irradiation, V_D = -30 V, V_G = -15 V.

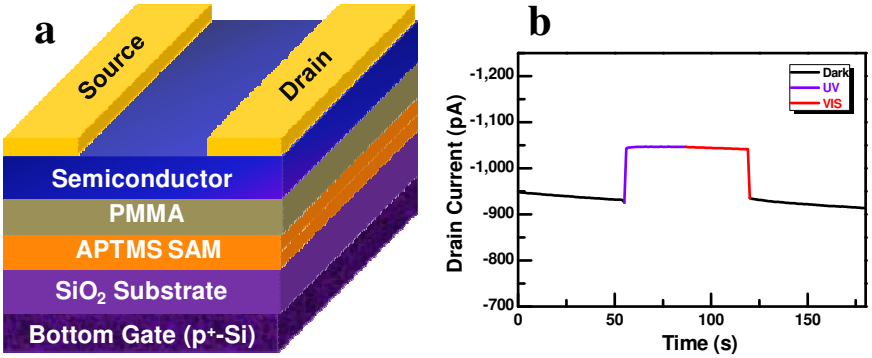

Figure S8. (a) Structural representation of a device built on APTMS-treated silicon substrates that were covered by PMMA thin films but lacks SP SAMs. (b) Time trace of the drain current for such a device under UV and visible light irradiation as a control, V_D = -30 V, V_G = -15 V.

References:

1. Guo, X. F.; Zhang, D. Q.; Zhang, H. J.; Fan, Q. H.; Xu, W.; Ai, X. C.; Fan, L. Z.; Zhu, D. B. *Tetrahedron* **2003**, *59*, 4843-4850.
2. Bunker, B. C.; Kim, B. I.; Houston, J. E.; Rosario, R.; Garcia, A. A.; Hayes, M.; Gust, D.; Picraux, S. T. *Nano Lett.* **2003,** *3*, 1723-1727.
3. Vlassiouk, I.; Park, C. D.; Vail, S. A.; Gust, D.; Smirnov, S. *Nano Lett.* **2006,** *6*, 1013-1017.
4. Stenger, D. A.; Georger, J. H.; Dulcey, C. S.; Hickman, J. J.; Rudolph, A. S.; Nielsen, T. B.; McCort, S. M.; Calvert, J. M. *J. Am. Chem. Soc.* **1992,** *114*, 8435-8442.